RESEARCH

Aberrant tryptophan metabolism in stromal cells is associated with mesenteric fibrosis in small intestinal neuroendocrine tumors

Anela Blažević[1], Anand M Iyer[1], Marie-Louise F van Velthuysen[2], Johannes Hofland[1], Peter M van Koestveld[1], Gaston J H Franssen[3], Richard A Feelders[1], Marina Zajec[4], Theo M Luider[4], Wouter W de Herder[1] and **Leo J Hofland[1]**

[1]Department of Internal Medicine, Section Endocrinology, Erasmus University Medical Center and Erasmus MC Cancer Institute, Rotterdam, Netherlands
[2]Department of Pathology, Erasmus University Medical Center and Erasmus MC Cancer Institute, Rotterdam, Netherlands
[3]Department of Surgery, Erasmus University Medical Center and Erasmus MC Cancer Institute, Rotterdam, Netherlands
[4]Laboratory of Neuro-Oncology/Clinical & Cancer Proteomics, Department of Neurology, Erasmus University Medical Center and Erasmus MC Cancer Institute, Rotterdam, Netherlands

Correspondence should be addressed to A Blazevic: a.blazevic.1@erasmusmc.nl

Abstract

Background: Increased levels of serotonin secretion are associated with mesenteric fibrosis (MF) in small intestinal neuroendocrine tumors (SI-NETs). However, the profibrotic potential of serotonin differs between patients, and in this study, we aimed to gain an understanding of the mechanisms underlying this variability. To this end, we analyzed the proteins involved in tryptophan metabolism in SI-NETs.
Methods: Proteomes of tumor and stroma from primary SI-NETs and paired mesenteric metastases of patients with MF (n = 6) and without MF (n = 6) were identified by liquid chromatography–mass spectrometry (LC-MS). The differential expression of proteins involved in tryptophan metabolism between patients with and without MF was analyzed. Concurrently, monoamine oxidase A (MAO-A) expression was analyzed in the tumor and stromal compartment by immunohistochemistry (IHC) and reported as intensity over area (I/A).
Results: Of the 42 proteins involved in tryptophan metabolism, 20 were detected by LC-MS. Lower abundance of ten proteins was found in mesenteric metastases stroma in patients with MF. No differential expression was found in primary SI-NETs. In patients with MF, IHC showed lower MAO-A expression in the stroma of the primary SI-NETs (median 4.2 I/A vs 6.5 I/A in patients without MF, $P = 0.003$) and mesenteric metastases (median 2.1 I/A vs 2.8 I/A in patients without MF, $P = 0.019$).
Conclusion: We found a decreased expression of tryptophan and serotonin-metabolizing enzymes in the stroma in patients with MF, most notably in the mesenteric stroma. This might account for the increased profibrotic potential of serotonin and explain the variability in the development of SI-NET-associated fibrotic complications.

Key Words
- neuroendocrine tumor
- mesenteric fibrosis
- proteomics
- immunohistochemistry
- tryptophan
- serotonin
- monoamine oxidase A

Endocrine Connections (2022) **11**, **e220020**

Introduction

Small intestinal neuroendocrine tumors (SI-NETs) are accompanied by specific clinical pathology, most notable carcinoid syndrome and fibrotic complications such as carcinoid heart disease and mesenteric fibrosis (MF) (1). There is a lack of medical treatment options to prevent or reduce symptoms, in particular, for fibrotic complications (2). Increased understanding of the pathobiology of these fibrotic complications is key to develop effective treatment options.

https://ec.bioscientifica.com
https://doi.org/10.1530/EC-22-0020

It is well established that SI-NETs secrete a wide array of bioactive molecules, with a central role for the bioamine serotonin (2, 3). Serotonin signaling is involved in various biological processes. Importantly, it can promote fibrosis development in various tissues (4). Serotonin production by SI-NETs is often measured on a systemic level by the urinary excretion of 5-hydroxyindoleacetic acid (5-HIAA), the main serotonin metabolite (5). Increased 5-HIAA urinary excretion in SI-NETs is associated with fibrotic complications. However, even though serotonin seems to be an important driver of SI-NET-associated fibrotic complications, several questions remain unanswered. First, it is unclear why certain locations, that is heart valves and mesentery, are more susceptible to the profibrotic effect of serotonin. Second, contrary to carcinoid heart disease, increased 5-HIAA excretion levels are a poor predictor for the individual risk of mesenteric fibrosis development (2, 6). Since 5-HIAA excretion levels do not necessarily correspond with local serotonin levels, this suggests an important role for paracrine serotonin signaling in SI-NET-associated mesenteric fibrosis (4).

We hypothesize that individual susceptibility for mesenteric fibrosis could be influenced by the local tumor microenvironment. Tryptophan metabolism is involved in the synthesis and catabolism of serotonin (7). Individual differences in this process could explain the variable risk for mesenteric fibrosis, as a decreased serotonin catabolism would result in increased serotonin signaling in the tumor microenvironment (8). To investigate this further, we analyzed the proteome of SI-NETs and their microenvironment in patients with and without MF for proteins involved in the tryptophan metabolism by liquid chromatography–mass spectrometry (LC-MS).

Methods

Sample selection

Patients were included from the Erasmus Medical Center NET database. The study was performed retrospectively, and, according to the guidelines of the Central Committee on Research involving Human Subjects, this does not require approval from an ethics committee in the Netherlands. Patients were selected for inclusion if they underwent a resection of a pathologically proven primary SI-NET with metastasectomy of the dominant mesenteric node at the Erasmus Medical Center between 2008 and 2016 (1). The dominant mesenteric node needed to be ≥10 mm on the short axis on a preoperative contrast-enhanced CT scan.

This group of 72 patients was assessed for mesenteric fibrosis on the preoperative CT scan and on 4-µm thick formalin-fixed, paraffin-embedded, hematoxylin and eosin (HE)-stained sections of the largest mesenteric metastasis. Radiological MF was defined as the presence of radiating soft-tissue strands in the mesentery and no radiological MF was defined as no radiating strands of soft-tissue visible on CT scan. Histological assessment classified mesenteric metastases with intratumoral fibrous bands >2 mm as severe MF while those with intratumoral fibrous bands <0.5 mm were classified as non-MF (9). Patients were included in the MF group ($n=6$) if there was radiological evidence for MF and severe MF on histological assessment. As sex is correlated with the risk of mesenteric disease, we selected an equal number of male and female patients (10). The non-MF group consisted of matched patients (age, sex and tumor grade according to World Health Organization, $n=6$) without MF on radiological and histological assessment.

Sample collection and data acquisition

Formalin-fixed paraffin-embedded (FFPE) tissue samples of the primary tumor and mesenteric metastasis from the first intestinal resection with mesenteric metastectomy were selected. Sections of 10 µm were attached to a polyethylene naphthalate slide (Carl Zeiss MicroImaging, Munich, Germany) and HE stained. The tissue samples were collected as described previously (11). Briefly, the tissue samples were separated by laser capture microdissection in tumor and stromal components using Zeiss PALM MicroBeam IV LCM microscope (Carl Zeiss MicroImaging, GmbH). This resulted in four samples for each patient: tumor cells of primary tumor, tumor cells of mesenteric metastasis, stromal cells of primary tumor and stromal cells of mesenteric metastasis. For each sample, an area of ~ 2 mm^2 that corresponds to ~20,000 cells was collected in a 0.5 mL opaque AdhesiveCap tube (Carl Zeiss MicroImaging). Following collection, the microdissected samples were dissolved in 20 µL of 0.1% RapiGest SF (Waters, Milford, MA, USA) and transferred into LoBind Eppendorf tubes (Eppendorf AG, Hamburg, Germany) and were digested with trypsin. LC-MS measurements were performed on an RSLC nano LC system (Thermo Fisher Scientific) coupled to an Orbitrap Fusion Tribrid Mass Spectrometer (Thermo Fisher Scientific) as described previously (12). Briefly, 10 µL of digest was loaded onto a trap column (C18 $PepM^{12}ap$, 300 µm ID x 5 mm, 5 µm, 100 Å) and desalted for 10 min using 0.1% TFA at a flow rate of 20 µL/min. Trap column was switched in-line with an analytical column (PepMap C18,

https://ec.bioscientifica.com
https://doi.org/10.1530/EC-22-0020

75 µm ID x 250 mm, 2 µm, 100 Å) and peptides were eluted using a binary 90´ gradient increasing solvent B from 4 to 38%, whereby solvent A was 0.1% formic acid, solvent B 80% acetonitrile and 0.08% formic acid, flow rate 300 nL/min and column temperature 40°C. For electrospray ionization, nano ESI emitter (New Objective) was used and a spray voltage of 1.7 kV was applied. A data-dependent acquisition MS method was used with an orbitrap survey scan (range 375–1500 m/z, 120,000 resolution, AGC target 400,000), followed by consecutive isolation, fragmentation (HCD, 30% NCE) and detection (ion trap, AGC 10,000) of the peptide precursors detected in the survey scan until a duty cycle time of 3" was exceeded ('Top Speed' method). Precursor masses that were selected once for MS/MS were excluded for subsequent fragmentation for 60". Acquired data has been made publicly available through the ProteomeXchange Consortium using the PRIDE identifier PXD029979 (13). MS/MS spectra from the raw data files of each sample were converted into MGF files using ProteoWizard (version 3.0). MGF peak list files were used to carry out searches using Mascot (version 2.3.02) against the Uniprot database (selected for *Homo sapiens*, downloaded 15 November 2015, 20,194 entries). Carbamidomethylation (+57 Da) of cysteine was set as the fixed modification and hydroxylations (+16 Da) of proline, lysine, and methionine were included as variable modifications. Mascot search results were further analyzed in Scaffold (v4.6.2, Portland, OR, USA) with protein confidence levels set to a 1% false discovery rate (FDR), at least two peptides per protein, and a 1% FDR at the peptide level. FDRs were estimated by inclusion of a decoy database search generated by Mascot. A Protein Report exported from Scaffold was used for data analysis. To analyze the components of tryptophan metabolism, the identified proteins were cross-referenced with genes from the tryptophan metabolism pathway hsa00380 of the Kyoto Encyclopedia of Genes and Genomes (KEGG) pathway database (http://www.genome.jp/kegg/pathway.html).

Validation of monoamine oxidase A expression

Immunohistochemistry (IHC) for monoamine oxidase A (MAO-A) was performed on FFPE whole sections of all the analyzed primary tumors and mesenteric metastases. Sequential 4 µm thick FFPE sections were stained for MAO-A (EPR7101, ab126751, 1:3200, Abcam) by automated IHC using the Ventana Benchmark ULTRA (Ventana Medical Systems Inc.). In brief, following deparaffinization and heat-induced antigen retrieval with CC1 (no. 950-500, Ventana) for 64 min the tissue samples were incubated with the antibody of interest for 32 min at 37°C. The staining was developed using Optiview universal DAB detection Kit (no. 760-700, Ventana), followed by hematoxylin II counterstain for 8 min and then a blue coloring reagent for 8 min according to the manufacturer's instructions (Ventana). Positive controls were used on every slide.

Immunohistochemically stained samples were digitalized and four fields of view were representatively selected. Each field of view was exported as an image file on a 10× magnification scale and contained both tumor cells and stroma. The exported images were analyzed using the CellProfiler software (version 3.0, www.cellprofiler.org) (14). Each image was manually segmented into the tumor and stromal compartments and the average intensity of DAB staining of the segmented area (I/A) was noted.

Statistics

Baseline patient characteristics and IHC data were presented as a median with interquartile range (IQR; 25th–75th percentiles) or as a percentage with count. Differential protein expression between MF and non-MF samples of the four groups (tumor cells of primary tumor, tumor cells of mesenteric metastasis, stromal cells of primary tumor and stromal cells of mesenteric metastasis) was determined using the spectral index (SpI) calculation. SpI is a metric calculated by the abundance of spectral counts in each group relative to the number of samples in which it is detectable. We have used SpI as it has a higher sensitivity to detect differential protein expression compared to several other methods (15). The significance of a given SpI is determined by permutation testing of the whole dataset (15). In our study, an FDR of 1% corresponded with the absolute SpI threshold of 0.60. Continuous data were compared by using a Mann–Whitney *U* test or Wilcoxon signed-rank test for paired data. A *P*-value of <0.05 was considered statistically significant.

Results

Dataset characteristics

For this study, 12 SI-NET patients were included. The baseline characteristics are shown in Table 1. There were no significant differences between the MF and non-MF patients with respect to age, sex, tumor grade, urinary 5-HIAA excretion, ENETS disease stage or preoperative medical treatment.

https://ec.bioscientifica.com
https://doi.org/10.1530/EC-22-0020

Table 1 Baseline characteristics.

	MF ($n = 6$)	**Non-MF** ($n = 6$)	***P*-value**
Median age (IQR), years	56 (49–65)	56 (49–61)	0.99
Female, *n* (%)	3 (50)	3 (50)	1.00
Tumor grade 1	6 (100%)	6 (100%)	1.00
Median urinary 5-HIAA (IQR) – µmol/24 h	150 (68–1299)	60 (49–103)	0.57
ENETS disease stage – *n* (%)			0.25
Stage III	2 (33)	4 (67)	
Stage IV	4 (67)	2 (33)	
Preoperative treatment, *n* (%)			0.22
None	3 (50)	5 (83)	
2003SSA	3 (50)	1 (17)	
Surgery indication, *n* (%)			0.26
Curative	1 (17)	4 (67)	
Palliative – prophylactic	3 (50)	2 (33)	
Palliative – symptomatic	2 (33)	N/A	

5-HIAA, urinary 5- hydroxyindoleacetic acid excretion, normal range <50 µmol/24 h, SSA, somatostatin analog.

LC-MS analysis of proteins involved in the tryptophan metabolism pathway

Proteomics analysis was performed on four samples of each patient, resulting in four groups: tumor cells of primary tumor, stroma of primary tumor, tumor cells of mesenteric metastasis and stroma of mesenteric metastasis. In the overall dataset, 2988 individual proteins could be identified. When compared to the 42 genes of the KEGG tryptophan metabolism pathway, we found 20 genes that coded for the proteins in our dataset (Supplementary Table 1, see section on supplementary materials given at the end of this article). Differential expression of proteins between MF and non-MF samples in each group was determined by SpI and yielded 10 differentially expressed proteins (Table 2). The differentially expressed proteins were mostly found in the tryptophan – serotonin metabolism and the fatty acid oxidation arm of the tryptophan metabolism pathway. In the kynurenine metabolism arm, only 3-hydroxyanthranilate 3,4-dioxygenase (HAAO) could be detected. All the differentially expressed proteins showed significantly lower abundance in fibrotic mesenteric stroma compared to non-fibrotic mesenteric stroma. Additionally, HAAO had a significantly lower abundance in fibrotic mesenteric tumor cells compared to non-fibrotic mesenteric tumor cells. No significant differential expression of the 20 selected proteins was observed between MF and non-MF samples in the primary tumor and stroma groups. Figure 1 shows a simplified diagram of the tryptophan metabolism pathway annotated with the identified and differentially expressed proteins in the mesenteric stroma samples.

Immunohistochemical analysis of monoamine oxidase A protein expression

We validated, by IHC staining, the expression of MAO-A, a key enzyme responsible for serotonin metabolism. Cytoplasmic staining was present in all primary tumors and mesenteric metastases, both in tumor cells and surrounding stroma. In the stromal compartment, MAO-A staining was predominantly expressed by fibroblasts (Fig. 2A). In primary tumors, the stromal compartment had a significantly lower staining score of MAO-A compared to tumor cells (median 5.5 I/A vs 28.3 I/A, respectively, $P < 0.001$). Similarly, in mesenteric metastases, the stromal MAO-A staining score was lower than in tumor cells (median 2.6 I/A vs 27.5 I/A, respectively, $P < 0.001$). Comparing the stromal compartment, MAO-A expression was lower in mesenteric metastases than in primary tumors (median 2.6 I/A vs 5.5 I/A, respectively, $P < 0.001$).

Next, we compared patients with and without mesenteric fibrosis (MF vs non-MF) (Fig. 2B). In primary tumors, patients with MF had higher MAO-A staining score in tumor cells (median 33.5 I/A vs 25.8 I/A in non-MF, $P = 0.03$). On the other hand, in the stromal compartment of primary tumors, the MAO-A staining score was lower in patients with MF (median 4.2 I/A vs 6.5 I/A in non-MF, $P = 0.003$). In mesenteric metastases, there was no difference in MAO-A staining score in MF and non-MF tumors cells (median 25.8 I/A vs 27.6 I/A, respectively, $P = 0.92$). Similar to the findings in primary tumors, MAO-A staining score in the stromal compartment of mesenteric metastases was lower in the MF samples (median 2.1 I/A vs 2.8 I/A in non-MF, $P = 0.019$). As more patients with MF received SSA treatment preoperatively compared to non-MF patients

https://ec.bioscientifica.com
https://doi.org/10.1530/EC-22-0020

Table 2 Results of spectral index analysis comparing fibrotic and non-fibrotic samples. Results of spectral index (SpI) analysis comparing fibrotic and non-fibrotic samples. SpI is calculated by the abundance of spectral counts in fibrotic samples and non-fibrotic samples (MF vs non-MF) relative to the number of samples in which it is detectable. A false discovery rate (FDR) of 1% corresponded with the absolute SpI threshold of 0.60.

Protein	Gene	Primary tumor		Mesenteric metastasis	
		Tumor	Stroma	Tumor	Stroma
Acetyl-CoA acetyltransferase, mitochondrial	*ACAT1*	0.01	0.29	−0.08	**−0.74**
Acetyl-CoA acetyltransferase, cytosolic	*ACAT2*	0.39	N/A	0.17	N/A
Aldehyde dehydrogenase X, mitochondrial	*ALDH1B1*	−0.27	0.14	−0.53	−0.33
Aldehyde dehydrogenase, mitochondrial	*ALDH2*	0.02	0.07	0.04	−0.36
Aldehyde dehydrogenase family 3 member A2	*ALDH3A2*	0.57	N/A	0.06	N/A
Alpha-aminoadipic semialdehyde dehydrogenase	*ALDH7A1*	0.13	−0.26	−0.08	−0.50
4-trimethylaminobutyraldehyde dehydrogenase	*ALDH9A1*	−0.02	−0.17	0.09	−0.58
Amiloride-sensitive amine oxidase	*AOC1*	0.32	−0.11	0.48	−0.59
Catalase	*CAT*	0.19	−0.36	0.12	**−0.83**
Aromatic-L-amino-acid decarboxylase	*DDC*	0.03	−0.05	−0.11	−0.52
Dihydrolipoyl dehydrogenase	*DLD*	0.14	0.15	−0.13	−0.50
Dihydrolipoyllysine-residue succinyltransferase component	*DLST*	0.02	0.16	0.16	**−0.83**
Enoyl-CoA hydratase, mitochondrial	*ECHS1*	0.12	−0.14	−0.04	**−0.67**
3-hydroxyanthranilate 3,4-dioxygenase	*HAAO*	0.26	0.48	**−0.63**	**−0.61**
Hydroxyacyl-coenzyme A dehydrogenase, mitochondrial	*HADH*	0.19	−0.33	0.00	−0.17
Trifunctional enzyme subunit alpha, mitochondrial	*HADHA*	0.21	0.03	0.03	**−0.95**
Monoamine oxidase A	*MAOA*	0.29	−0.15	-0.04	**−0.67**
Monoamine oxidase B	*MAOB*	0.17	0.19	0.00	**−0.60**
2-oxoglutarate dehydrogenase, mitochondria	*OGDH*	0.31	0.33	0.12	**−0.83**
2-oxoglutarate dehydrogenase-like, mitochondrial.	*OGDHL*	0.41	0.23	0.15	**−0.67**

Values of ≤−0.60 or ≥0.60 were considered significantly differentially expressed (bold).

(Table 1, $P=0.22$), we analyzed if this affected MAO-A expression and found no significant differences between SSA treated and naive patients within the four tissue groups.

Discussion

We have studied the protein expression of metabolizing enzymes within the tryptophan pathway in primary SI-NETs and paired mesenteric metastases and found most notably a decreased expression of serotonin-metabolizing enzymes in the stroma of fibrotic mesenteric metastases.

Serotonin production outside the CNS is limited to enterochromaffin cells and in extension to SI-NETs, in case of malignant transformation. In other tissues, serotonin levels are regulated by serotonin-metabolizing enzymes (16). Serotonin is a well-established profibrotic factor and increased paracrine serotonin signaling is known to induce tissue fibrosis and tumor cell proliferation (3, 4). Lower levels of serotonin-metabolizing enzymes result in an increase of local serotonin levels (16). This could also explain the observation that urinary 5-HIAA excretion, a marker for systemic serotonin production, is a poor predictor for mesenteric fibrosis as it may not reflect local serotonin activity (6, 17). The lower abundance of serotonin-metabolizing enzymes found in this study could be a major factor contributing to the increased risk of mesenteric fibrosis in some SI-NET patients. Interestingly, we found lower levels of MAO-A, the primary catabolizing enzyme of serotonin, in stroma of mesenteric metastases compared to primary tumors. This may represent an important mechanism in the predisposition of SI-NET-associated fibrosis in specific locations such as the mesentery.

MAO-A expression can be regulated via various mechanisms. It is well established that *MAO-A* gene and promotor polymorphism can result in lower transcription efficiency and increased serotonin levels. However, MAO-A expression can also be affected by environmental and epigenetic events (18). Downregulation of MAO-A by epigenetic methylation and histone acetylation has been demonstrated in cholangiocarcinoma and hepatocellular carcinoma and was associated with increased invasiveness, low tumor differentiation and poor prognosis (19, 20). However, studies on the role of MAO-A in tumorigenesis have not been consistent. In contrast to hepatocellular and cholangiocarcinoma, increased expression of MAO-A in stromal fibroblasts in prostate cancer promotes tumorigenesis *in vitro* and *in vivo* (21). Furthermore,

https://ec.bioscientifica.com
https://doi.org/10.1530/EC-22-0020

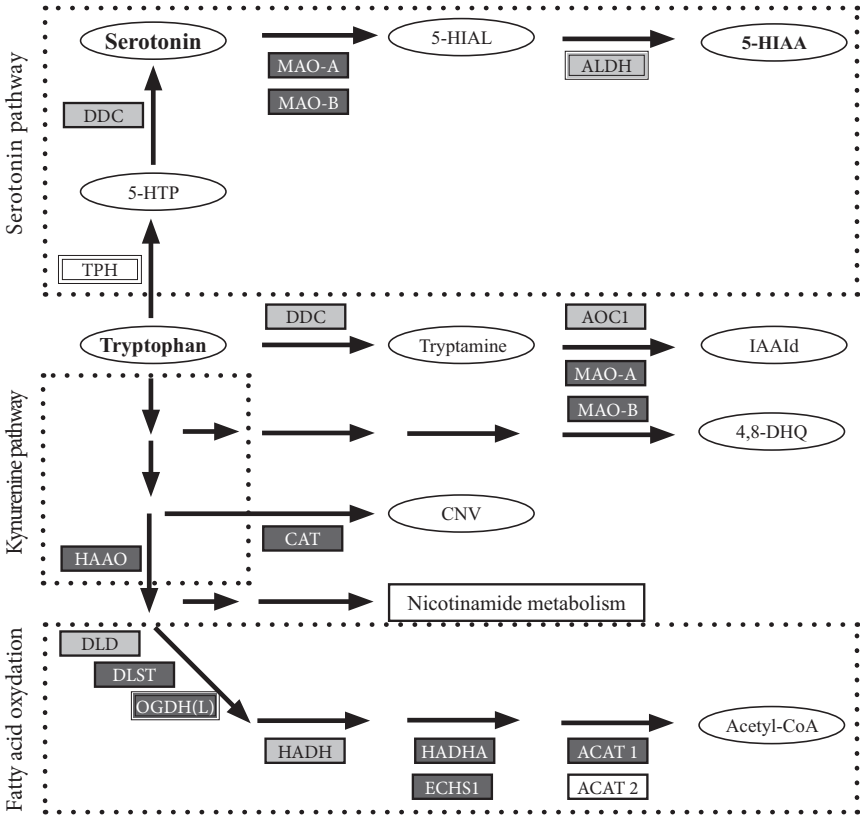

Figure 1
Simplified tryptophan metabolism pathway in mesenteric metastases stroma. Metabolites are shown as ellipses and enzymes as rectangles. Gray rectangles represent identified proteins and dark gray rectangles represent enzymes with significantly lower abundance in mesenteric metastases stroma of patients with mesenteric fibrosis. 4,8-DHG, 4,8-dihydroxy-quinoline; 5-HTP, 5-hydroxy- L-tryptophan; 5-HIAL, 5-hydroxyindole-acetylaldehyde; 5-HIAA, 5-hydroxyindoleacetic acid; ACAT1, acetyl-CoA acetyltransferase (mitochondrial); ACAT2, acetyl-CoA acetyltransferase (cytosolic); ALDH (multiple enzymes), aldehyde dehydrogenase X (mitochondrial); aldehyde dehydrogenase (mitochondrial); aldehyde dehydrogenase family 3 member A2; alpha-aminoadipic semialdehyde dehydrogenase and 4-trimethylaminobutyraldehyde dehydrogenase; AOC1, amiloride-sensitive amine oxidase; CAT, catalase; CNV, cinnavalininate; DDC, aromatic-L-amino-acid decarboxylase; DLD, dihydrolipoyl dehydrogenase (mitochondrial); DLST, dihydrolipoyllysine-residue succinyltransferase component of 2-oxoglutarate dehydrogenase complex (mitochondrial); ECHS1, enoyl-CoA hydratase (mitochondrial); HAAO, 3-hydroxyanthranilate 3,4-dioxygenase; HADH, hydroxyacyl-coenzyme A dehydrogenase (mitochondrial); HADHA, trifunctional enzyme subunit alpha (mitochondrial); IAAId, indole-3-acetaldehyde; MAO-A, monoamine oxidase A; MAO-B, monoamine oxidase B; OGDH(L), 2-oxoglutarate dehydrogenase and 2-oxoglutarate dehydrogenase-like (mitochondrial); TPH, tryptophan 5-hydroxylase 1 and 2.

increased MAO-A expression was suggested to play a role in non-small cell lung cancer by promoting epithelial to mesenchymal transition (22). These results suggest that the function of MAO-A varies in different cancer types warranting caution in the development of therapies targeting MAO-A.

Therapeutic targeting of MAO-A has predominantly focussed on the use of small molecule MAO inhibitors (MAOI), especially in the treatment of psychiatric and neurological disorders (23). Recent studies have demonstrated interesting novel effects of MAOI in cancer models. Inhibition of MAO-A activity by MAOI resulted in tumor suppression in preclinical mouse syngeneic and human xenograft tumor models. The antitumor effect was enhanced when MAOI was used in combination with immune checkpoint anti-PD-1 treatment (24). Also, MAO-A promotes tumor-associated macrophages' immunosuppressive functions via upregulation of oxidative stress which could be regulated by the use of MAOI resulting in enhanced antitumor immunity (25). However, relatively fewer options are as yet available to increase MAO-A expression or activity. Valproic acid (VPA), an anticonvulsant, was found to be an inducer of MAO-A activity through the Akt/FoxO1 signaling pathway (26). VPA may thus be a potential therapeutic option in regulating serotonin-mediated fibrosis in SI-NET. An additional benefit of VPA is its activity as a potent histone deacetylase inhibitor that has been demonstrated in NET cell lines to increase expression of somatostatin receptor 2 and have a cytotoxic effect (27, 28). However, the consequences of MAO-A inhibition vs induction on SI-NET tumor progression and fibrogenesis need to be investigated further.

Next to the proteins involved in the conversion to and degradation of serotonin, the tryptophan pathway consists of enzymes involved in the kynurenine metabolism and fatty acid oxidation. In the kynurenine pathway tryptophan is metabolized to nicotinamide adenosine

https://ec.bioscientifica.com
https://doi.org/10.1530/EC-22-0020

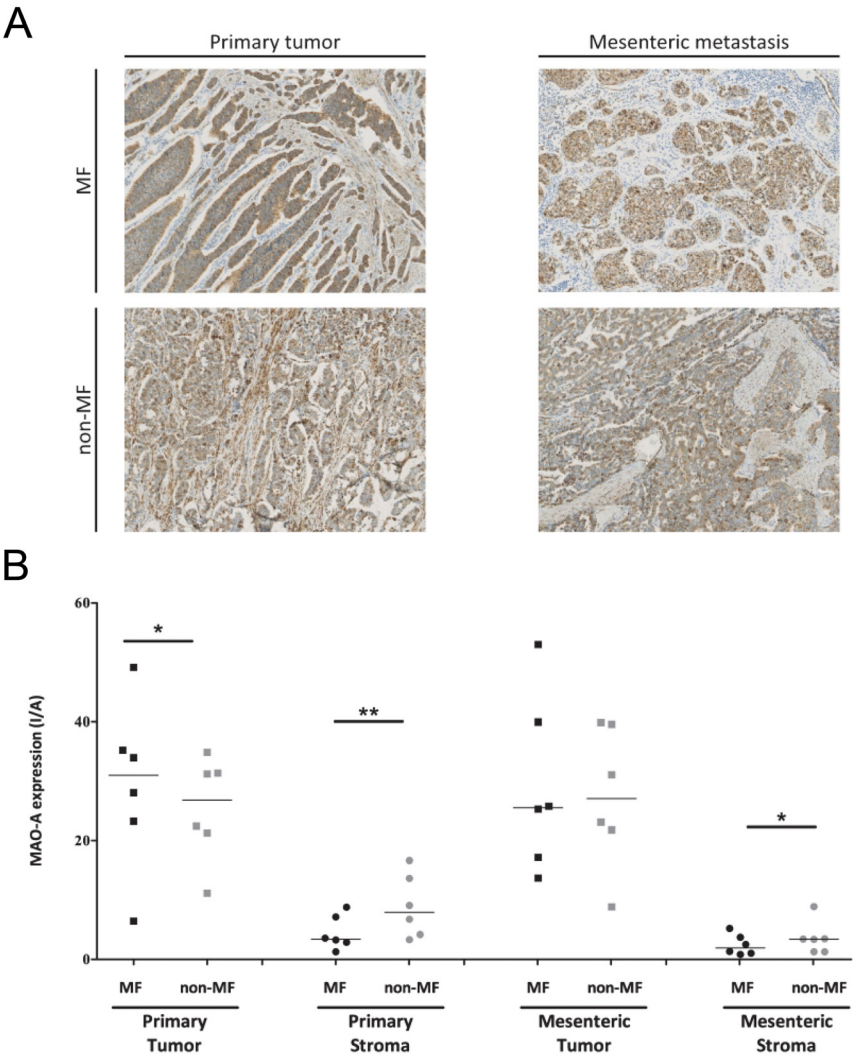

Figure 2
IHC analysis of MAO-A expression. (A) Photomicrographs of representative IHC staining for MAO-A. The left panel shows primary tumor tissue, the right panel shows mesenteric metastasis tissue. The upper panels shows tissue of patients with MF, the lower panels shows tissue of patients without mesenteric fibrosis (non-MF). (B) Median MAO-A expression in SI-NET patients with (MF, $n = 6$) and without (non-MF, $n = 6$) mesenteric fibrosis in primary tumor tumor cells, primary tumor stroma, mesenteric metastasis tumor cells and mesenteric metastasis stroma. MAO-A expression is scored as DAB intensity in segmented area (I/A). Each dot represents one individual patient with overall median indicated by the horizontal line. *$P < 0.05$, **$P < 0.01$ MF vs non-MF. IHC, immunohistochemical; MF, mesenteric fibrosis; MAO-A, monoamine oxidase A; SI-NET, small intestinal neuroendocrine tumors.

dinucleotide and is involved in the pathogenesis of many inflammatory and malignant diseases (29). Kynurenine metabolites have an immune suppressive effect resulting in a decreased antitumor immune response (29). On the other hand, this immunosuppressive effect has also been shown to attenuate fibrosis (30). In our study, we could only identify HAAO as part of the kynurenine pathway. Although this enzyme had a lower expression in both the fibrotic mesenteric tumor and stromal compartment, it is difficult to speculate the effect this could have on kynurenine metabolites and fibrogenesis in the SI-NET tumor microenvironment as most of the pathway could not be assessed.

On analyzing the arm of the tryptophan metabolism pathway involved in fatty acid oxidation, we were able to detect eight enzymes. These enzymes had a lower abundance in patients with mesenteric fibrosis, especially in the stroma of mesenteric metastases. Dysregulation of fatty acid metabolism is a common feature in cancer cells. Elevated exogenous uptake of fatty acids and subsequent oxidation allows for a valuable source of ATP and other molecules needed for proliferation in times of metabolic stress, such as hypoxia (31). Decreased fatty acid oxidation could result in increased reactive oxidative species production that results in profibrotic changes such as induction of myofibroblastic differentiation and increased transforming growth factor β (TGF-β) signaling (32).

This study has some limitations that may affect the conclusions drawn. As we have used a label-free proteomics approach not all proteins involved in the tryptophan metabolism could be detected. Notably, tryptophan hydroxylase 1, the rate-limiting enzyme for peripheral serotonin synthesis, was not detected. Secondly, using this approach the estimation of the abundance of the detected proteins is semi-quantitative. To overcome this limitation, we validated the expression of the main serotonin-

https://ec.bioscientifica.com
https://doi.org/10.1530/EC-22-0020

inactivating enzyme, MAO-A using IHC and found an identical pattern of decreased expression in mesenteric stroma as with the proteomics analysis. Thirdly, the small sample size is a major limitation of this study. Hence an in-depth investigation of the potential association of protein expression with disease characteristics was not possible. However, the altered expression of the enzymes involved in tryptophan metabolism demonstrated in this study may represent an important mechanism involved in mesenteric fibrosis in SI-NETs and warrants further research. Further in-depth studies involving larger sample populations could validate potential targets to develop effective treatment options for SI-NET-associated mesenteric fibrosis.

In conclusion, we found lower expression of enzymes involved in the tryptophan metabolism, especially serotonin-degrading enzymes, in the stroma of fibrotic mesenteric metastases. Differential expression of these enzymes might be an important factor underlying the risk of development of SI-NET-associated mesenteric fibrosis.

Supplementary materials

This is linked to the online version of the paper at https://doi.org/10.1530/EC-22-0020.

Declaration of interest

J H has received speaker and travel fees from Ipsen and Novartis and has joined the advisory board for Novartis. W H received research support from Ipsen and AAA/Novartis and received speaker fees from AAA/Novartis, Pfizer and Ipsen. R F is an Editorial Board Member of Endocrine Connections. He was not involved in the editorial or review process of this paper, on which he is a listed authors. The other authors have nothing to disclose.

Funding

This study has been supported by the Ipsen Fund via an unrestricted research fund.

References

1 Niederle B, Pape UF, Costa F, Gross D, Kelestimur F, Knigge U, Öberg K, Pavel M, Perren A, Toumpanakis C, *et al.* Enets consensus guidelines update for neuroendocrine neoplasms of the jejunum and ileum. *Neuroendocrinology* 2016 **103** 125–138. (https://doi.org/10.1159/000443170)

2 Koumarianou A, Alexandraki KI, Wallin G, Kaltsas G & Daskalakis K. Pathogenesis and clinical management of mesenteric fibrosis in small intestinal neuroendocine neoplasms: a systematic review. *Journal of Clinical Medicine* 2020 **9** 1777. (https://doi.org/10.3390/jcm9061777)

3 Blažević A, Hofland J, Hofland LJ, Feelders RA & de Herder WW. Small intestinal neuroendocrine tumours and fibrosis: an entangled conundrum. *Endocrine-Related Cancer* 2018 **25** R115–R130. (https://doi.org/10.1530/ERC-17-0380)

4 Mann DA & Oakley F. Serotonin paracrine signaling in tissue fibrosis. *Biochimica et Biophysica Acta* 2013 **1832** 905–910. (https://doi.org/10.1016/j.bbadis.2012.09.009)

5 Hofland J, Zandee WT & de Herder WW. Role of biomarker tests for diagnosis of neuroendocrine tumours. *Nature Reviews: Endocrinology* 2018 **14** 656–669. (https://doi.org/10.1038/s41574-018-0082-5)

6 Blazevic A, Zandee WT, Franssen GJH, Hofland J, van Velthuysen MF, Hofland LJ, Feelders RA & de Herder WW. Mesenteric fibrosis and palliative surgery in small intestinal neuroendocrine tumours. *Endocrine-Related Cancer* 2018 **25** 245–254. (https://doi.org/10.1530/ERC-17-0282)

7 Roth W, Zadeh K, Vekariya R, Ge Y & Mohamadzadeh M. Tryptophan metabolism and gut-brain homeostasis. *International Journal of Molecular Sciences* 2021 **22** 2973. (https://doi.org/10.3390/ijms22062973)

8 Shih JC, Chen K & Ridd MJ. Monoamine oxidase: from genes to behavior. *Annual Review of Neuroscience* 1999 **22** 197–217. (https://doi.org/10.1146/annurev.neuro.22.1.197)

9 Pantongrag-Brown L, Buetow PC, Carr NJ, Lichtenstein JE & Buck JL. Calcification and fibrosis in mesenteric carcinoid tumor: CT findings and pathologic correlation. *American Journal of Roentgenology* 1995 **164** 387–391. (https://doi.org/10.2214/ajr.164.2.7839976)

10 Blažević A, Iyer AM, van Velthuysen M-LF, Hofland J, Oudijk L, de Herder WW, Hofland LJ & Feelders RA. Sexual dimorphism in small-intestinal neuroendocrine tumors: lower prevalence of mesenteric disease in premenopausal women. *Journal of Clinical Endocrinology and Metabolism* 2022 dgac001. (https://doi.org/10.1210/clinem/dgac001)

11 Zajec M, Kros JM, Dekker-Nijholt DAT, Dekker LJ, Stingl C, van der Weiden M, van den Bosch TPP, Mustafa DAM & Luider TM. Identification of blood-brain barrier-associated proteins in the human brain. *Journal of Proteome Research* 2021 **20** 531–537. (https://doi.org/10.1021/acs.jproteome.0c00551)

12 van der Ende EL, Meeter LH, Stingl C, van Rooij JGJ, Stoop MP, Nijholt DAT, Sanchez-Valle R, Graff C, Öijerstedt L, Grossman M, *et al.* Novel CSF biomarkers in genetic frontotemporal dementia identified by proteomics. *Annals of Clinical and Translational Neurology* 2019 **6** 698–707. (https://doi.org/10.1002/acn3.745)

13 Vizcaíno JA, Côté RG, Csordas A, Dianes JA, Fabregat A, Foster JM, Griss J, Alpi E, Birim M, Contell J, *et al.* The proteomics IDEntifications (PRIDE) database and associated tools: status in 2013. *Nucleic Acids Research* 2013 **41** D1063–D1069. (https://doi.org/10.1093/nar/gks1262)

14 Carpenter AE, Jones TR, Lamprecht MR, Clarke C, Kang IH, Friman O, Guertin DA, Chang JH, Lindquist RA, Moffat J, *et al.* CellProfiler: image analysis software for identifying and quantifying cell phenotypes. *Genome Biology* 2006 **7** R100. (https://doi.org/10.1186/gb-2006-7-10-r100)

15 Fu X, Gharib SA, Green PS, Aitken ML, Frazer DA, Park DR, Vaisar T & Heinecke JW. Spectral index for assessment of differential protein expression in shotgun proteomics. *Journal of Proteome Research* 2008 **7** 845–854. (https://doi.org/10.1021/pr070271+)

16 Mohammad-Zadeh LF, Moses L & Gwaltney-Brant SM. Serotonin: a review. *Journal of Veterinary Pharmacology and Therapeutics* 2008 **31** 187–199. (https://doi.org/10.1111/j.1365-2885.2008.00944.x)

17 Laskaratos FM, Diamantopoulos L, Walker M, Walton H, Khalifa M, El-Khouly F, Koffas A, Demetriou G, Caplin M, Toumpanakis C, *et al.* Prognostic factors for survival among patients with small bowel neuroendocrine tumours associated with mesenteric desmoplasia. *Neuroendocrinology* 2018 **106** 366–380. (https://doi.org/10.1159/000486097)

18 Naoi M, Riederer P & Maruyama W. Modulation of monoamine oxidase (MAO) expression in neuropsychiatric disorders: genetic and environmental factors involved in type A MAO expression. *Journal of Neural Transmission* 2016 **123** 91–106. (https://doi.org/10.1007/s00702-014-1362-4)

19 Li J, Yang XM, Wang YH, Feng MX, Liu XJ, Zhang YL, Huang S, Wu Z, Xue F, Qin WX, *et al.* Monoamine oxidase A suppresses hepatocellular

carcinoma metastasis by inhibiting the adrenergic system and its transactivation of EGFR signaling. *Journal of Hepatology* 2014 **60** 1225–1234. (https://doi.org/10.1016/j.jhep.2014.02.025)

20 Huang L, Frampton G, Rao A, Zhang KS, Chen W, Lai JM, Yin XY, Walker K, Culbreath B, Leyva-Illades D, *et al.* Monoamine oxidase A expression is suppressed in human cholangiocarcinoma via coordinated epigenetic and IL-6-driven events. *Laboratory Investigation* 2012 **92** 1451–1460. (https://doi.org/10.1038/labinvest.2012.110)

21 Li J, Pu T, Yin L, Li Q, Liao CP & Wu BJ. MAOA-mediated reprogramming of stromal fibroblasts promotes prostate tumorigenesis and cancer stemness. *Oncogene* 2020 **39** 3305–3321. (https://doi.org/10.1038/s41388-020-1217-4)

22 Liu F, Hu L, Ma Y, Huang B, Xiu Z, Zhang P, Zhou K & Tang X. Increased expression of monoamine oxidase A is associated with epithelial to mesenchymal transition and clinicopathological features in non-small cell lung cancer. *Oncology Letters* 2018 **15** 3245–3251. (https://doi.org/10.3892/ol.2017.7683)

23 Finberg JPM & Rabey JM. Inhibitors of MAO-A and MAO-B in psychiatry and neurology. *Frontiers in Pharmacology* 2016 **7** 340. (https://doi.org/10.3389/fphar.2016.00340)

24 Wang X, Li B, Kim YJ, Wang YC, Li Z, Yu J, Zeng S, Ma X, Choi IY, Di Biase S, *et al.* Targeting monoamine oxidase A for T cell-based cancer immunotherapy. *Science Immunology* 2021 **6** eabh2383. (https://doi.org/10.1126/sciimmunol.abh2383)

25 Wang YC, Wang X, Yu J, Ma F, Li Z, Zhou Y, Zeng S, Ma X, Li YR, Neal A, *et al.* Targeting monoamine oxidase A-regulated tumor-associated macrophage polarization for cancer immunotherapy. *Nature Communications* 2021 **12** 3530. (https://doi.org/10.1038/s41467-021-23164-2)

26 Wu JB & Shih JC. Valproic acid induces monoamine oxidase A via Akt/forkhead box O1 activation. *Molecular Pharmacology* 2011 **80** 714–723. (https://doi.org/10.1124/mol.111.072744)

27 Veenstra MJ, van Koetsveld PM, Dogan F, Farrell WE, Feelders RA, Lamberts SWJ, de Herder WW, Vitale G & Hofland LJ. Epidrug-induced upregulation of functional somatostatin type 2 receptors in human pancreatic neuroendocrine tumor cells. *Oncotarget* 2018 **9** 14791–14802. (https://doi.org/10.18632/oncotarget.9462)

28 Arvidsson Y, Johanson V, Pfragner R, Wängberg B & Nilsson O. Cytotoxic effects of valproic acid on neuroendocrine tumour cells. *Neuroendocrinology* 2016 **103** 578–591. (https://doi.org/10.1159/000441849)

29 Chen Y & Guillemin GJ. Kynurenine pathway metabolites in humans: disease and healthy States. *International Journal of Tryptophan Research* 2009 **2** 1–19. (https://doi.org/10.4137/ijtr.s2097)

30 Dolivo DM, Larson SA & Dominko T. Tryptophan metabolites kynurenine and serotonin regulate fibroblast activation and fibrosis. *Cellular and Molecular Life Sciences* 2018 **75** 3663–3681. (https://doi.org/10.1007/s00018-018-2880-2)

31 Koundouros N & Poulogiannis G. Reprogramming of fatty acid metabolism in cancer. *British Journal of Cancer* 2020 **122** 4–22. (https://doi.org/10.1038/s41416-019-0650-z)

32 Li X, Zhang W, Cao Q, Wang Z, Zhao M, Xu L & Zhuang Q. Mitochondrial dysfunction in fibrotic diseases. *Cell Death Discovery* 2020 **6** 80. (https://doi.org/10.1038/s41420-020-00316-9)

Received in final form 3 March 2022
Accepted 10 March 2022
Accepted Manuscript published online 10 March 2022